

Nonlinear Control of UPFC in Power System for Damping Inter Area Oscillations

¹M.Praveen Kumar, ²P B Chennaiah

¹EEE, M.Tech student, AITS, Rajampet, Kadapa, A.P, India,

²EEE, Associate Professor, AITS, Rajampet, Kadapa, A.P, India,

Abstract: This paper introduces a new nonlinear control of flexible ac transmission systems (FACTS) controllers for the purpose of damping interarea oscillations in power systems. FACTS controllers consist of series, shunt, or a combination of series-shunt devices which are interfaced with the bulk power system through injection buses. Controlling the angle of these buses can effectively damp low frequency interarea oscillations in the system. The proposed control method is based on finding an equivalent reduced affine nonlinear system for the network from which the dominant machines are extracted based on dynamic coherency. It is shown that if properly selected, measurements obtained from this subsystem of machines are sufficient inputs to the FACTS controllers to stabilize the power system. The effectiveness of the proposed method on damping interarea oscillations is validated on the 68 bus, 16 generator system of the New England/New York network.

IndexTerms: Coherent groups, dominant machines, flexible ac transmission systems (FACTS), interarea oscillation, nonlinear control, phasor measurement unit (PMU), wide-area control.

I. INTRODUCTION

AS high voltage power electronics become less expensive and have a wider-range of operation, flexible ac transmission systems (FACTS) controllers will become more prevalent in the transmission system to control active power flow across congested corridors and ensure voltage security. In addition, FACTS controllers can provide promising solutions to many of the stability problems that occur within the bulk power system. FACTS controllers can be categorized into three major groups: shunt devices such as the Static Synchronous Compensator (STATCOM), series devices such as the static synchronous series compensator (SSSC) and series shunt devices such as the unified power flow controller (UPFC). In addition to steady-state solutions such as power flow and voltage control, an added benefit of FACTS controllers deployed in the transmission system is that they can also effectively control active power oscillations that can damage generators, increase line losses, and increase wear and tear on network components.

Therefore developing suitable control strategies is a requirement before FACTS can be confidently utilized in the power system. Several authors have investigated utilizing FACTS, especially UPFCs to damp interarea oscillations using a variety of control approaches [1]–[10]. Interarea oscillations can occur in a system because of contingencies such as sudden load changes or faults. In [1]–[5], oscillation damping is based on a linear control approach to the UPFC and power system, whereas other authors consider nonlinear control systems theory and Lyapunov Energy Functions [6]–[10]. Typically, nonlinear approaches are more effective for large perturbations or when the power system state strays significantly from the initial operating point.

The approach proposed in this paper provides a general nonlinear method for using multiple FACTS controllers in a power network for the purpose of damping interarea oscillations. In this paper, it is shown that any FACTS device capable of changing its interface bus angle(s) with the network can be used to mitigate power system oscillations. Using this method, it will be shown that both shunt and series FACTS controllers can be used for this purpose. The control method is based on finding a reduced nonlinear affine state space system for the network which can be controlled by feedback of selected measurements of rotor frequencies. While frequency measurements (such as from FNET [11]) have made wide area control of the power networks feasible, it is still not reasonable to expect that the full set of frequency measurements is available for controller use. Therefore, an approach is proposed to use a reduced set of measurements from a subset of machines in the system.

II. UPFC MODEL

The UPFC is the most versatile FACTS device. It consists of a combination of a shunt and series branches connected through the DC capacitor as shown in Fig. 1. Models for the STATCOM and SSSC can be easily extracted from the UPFC model by considering the shunt and series converters individually. The series connected inverter injects a voltage with controllable magnitude and phase angle in series with the transmission line, therefore providing active and reactive power to the transmission line. The shunt-connected inverter

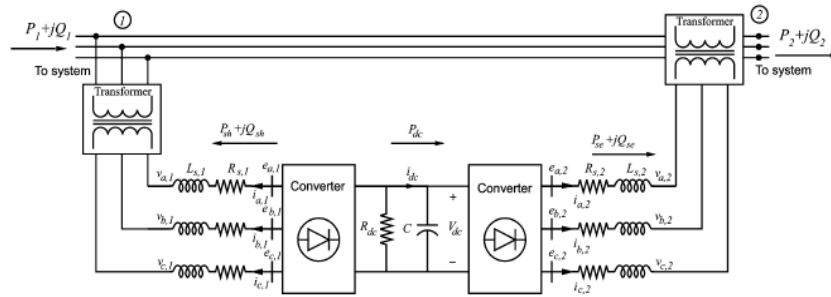


Fig. 1. Unified power flow controller diagram.

Provides the active power drawn by the series branch plus the losses and can independently provide reactive compensation to the system. The UPFC model is given by [12] as shown in (1)–(5) at the bottom of the next page, where the parameters are as shown in Fig. 1. The currents i_{d1} and i_{q1} are the dq components of the shunt current. The currents i_{d2} and i_{q2} are the dq components of the series current. The voltages $V1\angle\theta1$ and $V2\angle\theta2$ are the sending end and receiving end voltage magnitudes and angles, respectively. The UPFC is controlled by varying the phase angles ($\alpha1, \alpha2$) and ($k1, k2$) magnitudes of the converter shunt and series output voltages ($e1, e2$), respectively.

The power balance equations at bus 1 are given by

$$0 = V1((id1 - id2) \cos \theta1 + (iq1 - iq2) \sin \theta1) - V1 \sum_{j=1}^n VjY1j \cos(\theta1 - \thetaj - \phi1j) \dots \dots \dots (1)$$

$$0 = V1((id1 - id2) \sin \theta1 - (iq - iq2) \cos \theta1) - V1 \sum_{j=1}^n VjY1j \sin[(\theta1 - \thetaj - \phi1j)] \dots \dots \dots (2)$$

and at bus 2

$$0 = V2(id2 \cos \theta2 + iq2 \sin \theta2) - V2 \sum_{j=1}^n VjY2j \cos[(\theta2 - \thetaj - \phi2j)] \dots \dots \dots (3)$$

$$0 = V2(id2 \sin \theta2 + iq2 \cos \theta2) - V2 \sum_{j=1}^n VjY2j \sin[(\theta2 - \thetaj - \phi2j)] \dots \dots \dots (4)$$

III. SYSTEM MODEL

For control development purposes, several initial assumptions are made. The first assumption is that the system loads are modeled as constant impedance loads and can therefore be absorbed into the bus admittance matrix. Second, the generators are modeled as the classical “transient reactance behind constant voltage” model. Note that these assumptions are for control development *only*—the proposed control is validated with the full nonlinear 10-th order power system model given in the Appendix [13]. In addition, the proposed control is developed for the UPFC; control development for the STATCOM and SSSC follows a similar procedure and is therefore not explicitly detailed.

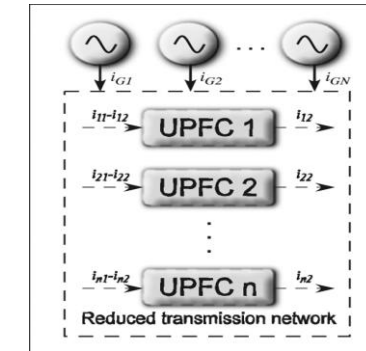


Fig. 2. Equivalent power system from the controller viewpoint.

Using the load impedance model, the only points of current injection into the network are the generator internal buses and the UPFC sending and receiving end buses. Using Kron reduction, the transmission network can be reduced to an admittance matrix of size $(N + n \times N + n)$ where N is the number of generator buses and n is the number FACTS current injections in the system. Fig. 2 illustrates the reduced system showing the points of current injection. Each UPFC has two current injections $i1$ and $i2$, at the sending and receiving ends, respectively; a STATCOM and SSSC have only one current. The generator current injections are given by i^G .

The classical model for the reduced network including the UPFCs.

Mechanical power, inertia constant and angular speed, respectively, of machine; and is synchronous speed. The summation represents the active power injected at each current injection point, including FACTS buses.

IV. CONTROLLER DESIGN

The controller design consists of three stages.

A. Stage I

The objective of the first design stage is to find the desired changes in mechanical powers required to stabilize the system. To obtain the amount of mechanical power required, it is initially assumed that the mechanical powers PMj , are inputs into the system model. Note that this is *only* for controller development; in the final control, it is not required that the generator mechanical powers actually vary.

Under this assumption, the system models are

$$\dot{x} = F(x) + GU \dots \dots \dots (5)$$

where as shown in (13)–(15) at the bottom of the page and $x = [\delta_1 \omega_1 \delta_2 \omega_2 \dots \dots \delta_N \omega_N]$.

Since it is only required that the system frequencies return to steady-state rapidly, a subset of (12) is

$$\dot{x} = f(x_1) + g u \dots\dots\dots(6)$$

where $x_1 = [\delta_1 \delta_2 \dots \dots \delta_N]$ and $x_2 = [\omega_1 \omega_2 \dots \omega_N]$

$$f(x_1) = \begin{bmatrix} -\frac{1}{M_1} E_1 \sum_{k=1}^{N+r} E_k Y_{1k} \cos(\delta_1 - \delta_k - \phi_{1k}) \\ \vdots \\ -\frac{1}{M_N} E_N \sum_{k=1}^{N+r} E_k Y_{Nk} \cos(\delta_N - \delta_k - \phi_{Nk}) \end{bmatrix} \dots(7)$$

where

$$g = \begin{bmatrix} \frac{1}{M_1} & \dots & 0 \\ \vdots & \ddots & \vdots \\ 0 & \dots & \frac{1}{M_1} \end{bmatrix} \dots\dots\dots(8)$$

$$u = [Pm_1 \ Pm_2 \ \dots \ Pm_n]$$

Letting x_{1s} , x_{2s} , and u_s denote the steady-state values of x_1 , x_2 and u , respectively, then the error in generator rotor frequencies becomes

$$e = x_2 - x_{2s} \dots\dots\dots(9)$$

and

$$\dot{e} = f(x) - f(x_{1s}) - g u_s + g u \dots\dots\dots(10)$$

Equation (21) can be stabilized with input u so that

$$u_d = g^{-1} [-f(x_1) + f(x_{1s}) - g u_s + K e] \dots\dots\dots(11)$$

where K is a positive definite matrix and

$$\dot{e} = -K e \dots\dots\dots(12)$$

B. Stage II

In Stage I, the required changes in the generator’s mechanical powers were found that stabilize the system. In Stage II, these changes are translated into control signals to the FACTS controllers. As noted previously, the generator mechanical powers do not actually change as a consequence of the proposed control. Therefore, using the desired active power changes, a new control signal is introduced

$$\Delta u = u_{desired} - u_{actual} \dots\dots\dots(13)$$

Where $u_{desired}$ and u_{actual} are the desired and actual values for the generator mechanical powers. This mismatch is translated into the desired changes in the FACTS’ bus voltage angles, as shown in (25) at the bottom of the page, where

$$L = [L_1, \dots, L_N]^T$$

$$\bar{\Delta} = [\Delta\delta_1, \dots, \Delta\delta_n]^T$$

The nonlinear system is solved numerically for $\bar{\Delta}$. Note that if $N \neq n$, then the system of equations is not square and an exact solution is not possible. In this case, the equations are solved to find the best fit to $\bar{\Delta}$ which minimizes the error. These values are then used to calculate the desired current injections i^*_{d1} , i^*_{q1} , i^*_{d2} , i^*_{q2} from the power balance (1)–(4).

C. Stage III

In Stage III, the desired current injections are translated into actual control values for the FACTS controllers. As before, this approach is developed for the UPFC only, noting that similar approaches can be developed for the SSSC and STATCOM. To find the actual control inputs, a predictive control based on [14] is used. The basic methodology of predictive control is to design an asymptotically stable controller such that in an

affine nonlinear system, the output $y(t)$ tracks a prescribed reference value $\omega(t)$ in terms of a given performance:

$$\dot{x} = f(x(t)) + g(x(t))u(t) \dots\dots\dots(14)$$

$$y_i(t) = h_i(x(t)) \quad i=1, \dots, m \dots\dots\dots(15)$$

Where m is the number of outputs equal to the number of inputs in $u(t)$. The receding horizon performance index is given by

$$J = \frac{1}{2} \int_0^T (\hat{y}(t + \tau) - \hat{\omega}(t + \tau))^2 d\tau \times (\hat{y}(t + \tau) - \hat{\omega}(t + \tau)) d\tau \dots\dots\dots(16)$$

where T is the predictive period. The actual control input $u(t)$ is given by the initial value of the optimal control input $\hat{u}(t + \tau)$ for $0 \leq \tau \leq T$ and $u(t + \tau)$ when $\tau = 0$.

The optimal predictive control law is given by

$$u(t) = -(L_g L_f^{\rho-1} h(x))^{-1} (K M_\rho + L_f^\rho h(x) - \omega^{(\rho)}(t)) \dots\dots\dots(17)$$

where ρ is the relative degree for the system outputs (assuming that all outputs have the same relative degree) and L is the Lie derivative defined by

$$L_\mu v = \frac{\partial v}{\partial x} \mu \dots\dots\dots(18)$$

The matrix K is given by

$$M_\rho = \begin{bmatrix} h(x) - w(t) \\ L_f^1 h(x) - w^{[1]}(t) \\ \vdots \\ L_f^{\rho-1} h(x) - w^{[\rho-1]}(t) \end{bmatrix} \dots\dots\dots(19)$$

The matrix K is the first rows of the matrix $\psi_{rr}^{-1} \psi_{pr}^T$ where

$$\psi_{rr} = \begin{bmatrix} \psi_{(\rho+1, \rho+1)} \dots \psi_{(\rho+1, \rho+r+1)} \\ \psi_{(\rho, \rho+1)} \dots \psi_{(\rho+r+1, \rho+r+1)} \end{bmatrix} \dots\dots\dots(20)$$

$$\psi_{pr} = \begin{bmatrix} \psi_{(1, \rho+1)} \dots \psi_{(1, \rho+r+1)} \\ \psi_{(\rho, \rho+1)} \dots \psi_{(\rho, \rho+r+1)} \end{bmatrix} \dots\dots\dots(21)$$

Where

$$\psi_{ij} = \frac{r^{i+j-1}}{(i-1)!(j-1)!(i+j-1)!}, \quad i, j=1, \dots, \rho+r+1 \dots\dots\dots(22)$$

And

$$\bar{T} = \text{diag}\{T, \dots, T\} \in R^{m \times m}$$

Returning to (1)–(5), the relative degree for all of the outputs is $\rho = 1$ and assuming the control order to be $r = 0$, then the control law for the UPFC becomes

$$u_1 = \frac{-3L_1}{\omega_s V_{dc} T} (i_{d1} - i_{d1}^*) + \frac{R_1}{V_{dc}} i_{d1} - \frac{L_1}{V_{dc}} \dot{i}_{q1} + \frac{V_1 \cos \theta_1}{V_{dc}} + \frac{L_1}{\omega_s V_{dc}} \frac{d}{dt} i_{d1}^* \dots\dots\dots(23)$$

$$u_2 = \frac{-3L_1}{\omega_s v_{dc} T} (i_{q1} - i_{q1}^*) + \frac{R_1}{V_{dc}} i_{q1} - \frac{L_1}{V_{dc}} \dot{i}_{d1} + \frac{V_1 \sin \theta_1}{V_{dc}} + \frac{L_1}{\omega_s v_{dc}} \frac{d}{dt} i_{q1}^* \dots\dots\dots(24)$$

$$u_3 = \frac{-3L_1}{\omega_s v_{dc} T} (i_{d2} - i_{d2}^*) + \frac{R_1}{V_{dc}} i_{d2} - \frac{L_1}{V_{dc}} \dot{i}_{q2} + \frac{V_2 \cos \theta_2}{V_{dc}} - \frac{V_1 \cos \theta_1}{V_{dc}} \frac{L_2}{\omega_s v_{dc}} \frac{d}{dt} i_{d2}^* \dots\dots\dots(25)$$

$$u_4 = \frac{-3L_2}{\omega_s v_{dc} T} (i_{q2} - i_{q2}^*) + \frac{R_2}{V_{dc}} i_{q2} - \frac{L_2}{V_{dc}} \dot{i}_{d2} + \frac{V_2 \sin \theta_2}{V_{dc}} - \frac{V_1 \sin \theta_1}{V_{dc}} + \frac{L_1}{\omega_s v_{dc}} \frac{d}{dt} i_{q1}^* \dots\dots\dots(26)$$

These inputs are then translated into the control inputs for the UPFC

$$k_1 = \sqrt{u_1^2 + u_2^2} \dots\dots\dots(27)$$

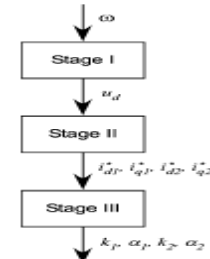


Fig. 3. Three stage control process.

$$\alpha_1 = \tan^{-1} \frac{u_2}{u_1} \dots\dots\dots(28)$$

$$k_2 = \sqrt{u_3^2 + u_4^2} \dots\dots\dots(29)$$

$$\alpha_2 = \tan^{-1} \frac{u_4}{u_3} \dots\dots\dots(30)$$

The three stage control process and outcomes of each stage are summarized in Fig.3

machines be ordered from 1 to Q and the rest of the machines be numbered from Q+1 to N, then the changes in the non-dominant machines can be approximated using a zero-th order model by

$$\begin{bmatrix} X_{Q+1,Q+1} & \dots & X_{Q+1,N} \\ \vdots & \ddots & \vdots \\ X_{N,Q+1} & \dots & X_{N,N} \end{bmatrix} \begin{bmatrix} \Delta\delta_{Q+1} \\ \vdots \\ \Delta\delta_N \end{bmatrix} = \begin{bmatrix} \sum_{k=1}^Q X_{Q+1,k} \Delta\delta_k - \sum_{k=N+1}^{N+n} X_{Q+1,k} \Delta\delta_k \\ \vdots \\ \sum_{k=1}^Q X_{N,k} \Delta\delta_k - \sum_{k=N+1}^{N+n} X_{N,k} \Delta\delta_k \end{bmatrix} \dots\dots(31)$$

Where

$$x_{ij} = \frac{\mu_{ij}}{\mu_{ii}} \dots\dots\dots(32)$$

And

$$\mu_{ij} = -E_i E_j Y_{ij} \sin(\delta_i - \delta_j - \varphi_{ij}) \quad i \neq j \dots\dots(33)$$

$$\mu_{ii} = -\sum_{k \neq i}^{N+n} E_i E_j Y_{ij} \sin(\delta_i - \delta_j - \varphi_{ij}) \quad i=j \dots\dots\dots(34)$$

Note that when only the dominant machines are selected for the control action, only the rows corresponding to the dominant machines will be used thereby reducing the order of the system. This is advantageous since the pseudo-inverse required to solve the set of equations is more nearly square providing better convergence.

VI. EXAMPLE AND RESULTS

Although the control has been developed using the classical generator model, the control approach will be validated using the full 10th order model which includes an exciter/AVR, turbine, and governor dynamics. The model is given in the Appendix. The proposed control is validated on the 68 bus, 16 generator New England/New York test system shown in Fig. 4. The coherent groupings corresponding to the five slowest modes are indicated by the dashed lines in Fig. 4. The network data and coherent groupings are the same as in [19]. The transmission tie lines are shown with bold lines. The reference generators for the five areas are G5, G13, G14, G15, and G16.

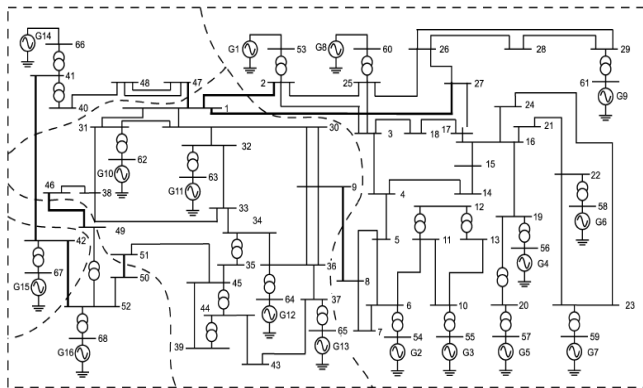


Fig. 4. The 68 bus, 16 generator test system

V. SELECTIVE FEEDBACK MEASUREMENTS BASED ON DOMINANT MACHINES

The control method proposed in the previous section requires generator rotor frequencies to be implemented. Although with recent advances in wide area frequency measurement (FNET) it may be possible to provide synchronized global measurements, it is still not feasible to assume that all generator rotor frequencies are simultaneously available. However, it is reasonable to assume that a subset of the measurements are available for feedback and the remainder of the states can be estimated based on the available measurements. The most probable machines to obtain measurements from are those machines which dominate coherent groups.

There are numerous methods for calculating coherent groups in the literature [15]–[18]. In [18], the coherency identification method is based on modal analysis and Gaussian elimination with full pivoting on the selected eigenvectors of the system to find the reference generators and their group members.

The selected eigenvectors are chosen based on the lowest oscillatory modes of the system. Once the dominant machines are found, a reduced order system is computed which captures the “slow” dynamics of the original system. In this process, the remaining unmeasured states of the system can be estimated based on the states which are measured via singular perturbation [13]. Let the dominant

TABLE I FACTS PARAMETERS

	R_1	L_1	R_2	L_2	R_p	C
UPFC	0.01	0.15	0.001	0.015	25	1400
STATCOMs	0.01	0.10	n/a	n/a	25	1200

Choosing the appropriate number of FACTS controllers in the network is based on the number of coherent areas. As a rule of thumb, it is best to match the number of current injections with the number of modes. For example, five current injections can be used to control the interarea oscillations between five areas. In the 68 bus example, four current injections are used: one UPFC (two injections) and two STATCOMS (one injection each). In this paper, the UPFC is placed on line 1–2 with the shunt converter on bus 2 and the STATCOMS have been placed on buses 47 and 49. The placements of the FACTS controllers were heuristically chosen to be at buses at the edge of the areas as might occur in practice. Several researchers have addressed the problem of optimal placement of FACTS controllers. In [20], the authors utilize modal sensitivity to determine placement of TCSCs. Eigenvalue shift is used as a placement strategy for SVCs in [21]. [22] focuses on the determination of the best bus placement for SVCs to damp interarea oscillations. Another recent work addresses the use of modal controllability indices specifically for FACTS placement for oscillation damping [23].

The parameters of the FACTS controllers are given in Table I. The per unit approach is the same as in [24] on a 100 MW, 100 kV base.

In the simulations, a solid three-phase fault is applied to bus 30 at 0.2 seconds and cleared at 0.3 seconds. The dynamic responses to this fault are shown for the following cases:

- Case 1) proposed control, all measurements available;
- Case 2) proposed control, only dominant machine measurements available;
- Case 3) linear control (taken from [25]).

Note that in Case 2), the estimation approach proposed in Section V is used to obtain approximations to the non-measured states.

Fig.5 shows a subset of the generator speeds with no FACTS controllers in the system compared to Case 1). Not all responses are shown for the sake of brevity. The selected generators are taken from four of the five coherent areas (generator 15 is by itself in an area and is not shown). Note that the generators go unstable as a result of the fault, but the proposed control is able to stabilize the system and rapidly mitigate the oscillations.

Fig. 6 shows the active power injections of the UPFC. The series injection is shown in the top figure and the shunt injection is shown in the bottom figure. In this figure, Case 2 (bold) is compared to Case 3 (thin). These series active power injection for the proposed control is very modest; therefore the rating of the series transformer and converter do not need to be overly large. The shunt active power is related to the series active power

$$-P_{shunt} = P_{series} - \frac{V_{dc}^2}{R_{dc}} \dots\dots\dots(35)$$

Therefore P_{shunt} will be opposite in polarity to P_{series} and will differ in magnitude by the losses in the converter. Furthermore, during transients the dc link capacitor will charge or discharge active power. Also note

that by definition, the shunt active power absorbed is positive, thus during steady-state the STATCOM will absorb active power and the figures indicate a positive value. The shunt converter injects active power into the system during the fault. Similar behavior is displayed by the STATCOMs as shown in Fig. 8. Fig. 9 shows the dc link capacitor voltages. The UPFC and one of the STATCOMs experience a drop of approximately 5% whereas the second STATCOM experiences a slight increase in voltage. This is reasonable, since to damp oscillations, it may be necessary to inject active power in some areas and absorb active power in other areas.

VII. CONCLUSIONS

A three stage nonlinear control scheme has been proposed for damping interarea oscillations using multiple FACTS controllers. Any FACTS device that can control its interface bu angle(s) with the power network can utilize this control approach. The method uses the generators' frequencies as the feedback data for the control. Using measurements from the dominant generators and estimating the rest of the states based on equivalent reduced systems is shown to considerably reduce the number of needed global measurements for control. Based on the simulation results, the proposed method shows promising results for wide-area control of power systems. There are several issues which need to be considered however.

There is a considerable computational burden for the controller which requires fast processors for real-time performance. However, good coherent groupings will lower the computation time by improving the estimation process. Future work will also consider the effect of time delays and communication noise in the measured states on the control effectiveness. Sensitivity of the proposed method to system uncertainties and topology changes will also be studied.

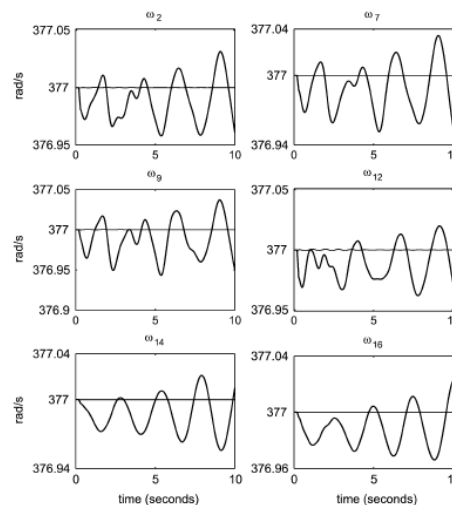


Fig. 5. Generator speeds for no FACTS controllers (bold) and Case 1 (thin).

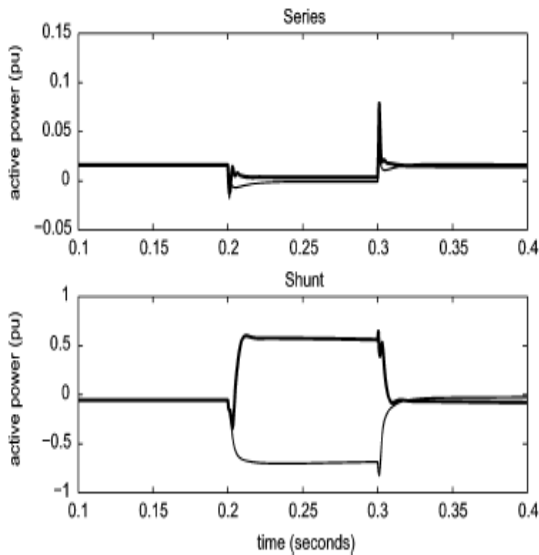


Fig. 6. UPFC injected active power: Series (top) and shunt (bottom); Case 2 (bold) and Case 3 (dashed).

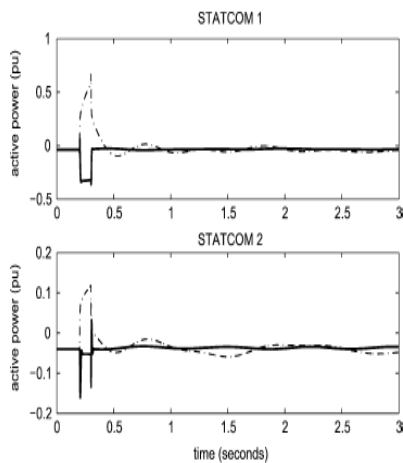


Fig. 7. STATCOM active power injection: Case 2 (bold), Case 3 (dashed).

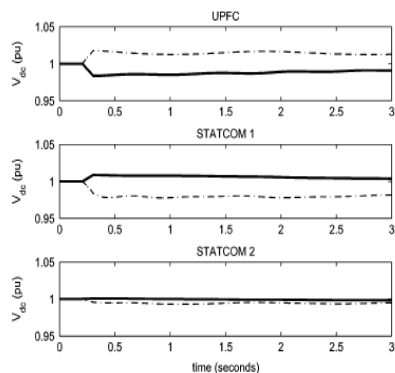


Fig. 8. FACTS Vdc: Case 2 (bold) and Case 3 (dashed).

REFERENCES

[1] H. Wang, "A unified model for the analysis of FACTS devices in damping power system oscillations—Part III: Unified power flow controller," *IEEE Trans. Power Del.*, vol. 15, no. 3, pp. 978–983, Jul. 2000.

- [2] B. C. Pal, "Robust damping of interarea oscillations with unified power flowcontroller," *Proc. Inst. Elect. Eng., Gen. Transm. Distrib.*, vol. 149, no. 6, pp. 733–738, Nov. 2002.
- [3] B. Chaudhuri, B. C. Pal, A. Zolotas, I. Jaimoukha, and T. Green, "Mixed-sensitivity approach to control of power system oscillations employing multiple FACTS devices," *IEEE Trans. Power Syst.*, vol. 18, no. 3, pp. 1149–1156, Aug. 2004.
- [4] M. M. Farsangi, Y. H. Song, and K. Y. Lee, "Choice of FACTS device control inputs for damping interarea oscillations," *IEEE Trans. Power Syst.*, vol. 19, no. 2, pp. 1135–1143, May 2004.
- [5] N. Tambey and M. L. Kothari, "Damping of power system oscillations with unified power flow controller (UPFC)," *Proc. Inst. Elect. Eng., Gen., Transm. Distrib.*, vol. 150, pp. 129–140, Mar. 2003.
- [6] M. Ghandhari, G. Andersson, and I. A. Hiskens, "Control Lyapunov functions for controllable series devices," *IEEE Trans. Power Syst.*, vol. 16, no. 4, pp. 689–694, Nov. 2001.
- [7] S. Robak, M. Januszewski, and D. D. Rasolomampionona, "Power system stability enhancement using PSS and Lyapunov-based controllers: A comparative study," in *Proc. IEEE Power Tech Conf., Bologna, Italy, 2003*, vol. 3, p. 6.
- [8] C.-C. Chu and H.-C. Tsai, "Application of Lyapunov-based adaptive neural network UPFC damping controllers for transient stability enhancement," presented at the *IEEE Power Energy Soc. General Meet., Pittsburgh, PA, Jul. 20–24, 2008*.
- [9] A. Bidadfar, M. Abedi, M. Karari, and C.-C. Chu, "Power swings damping improvement by control of UPFC and SMES based on direct Lyapunov method application," presented at the *IEEE Power and Energy Soc. General Meet., Pittsburgh, PA, Jul. 20–24, 2008*.
- [10] M. Januszewski, J. Machowski, and J. W. Bialek, "Application of the direct Lyapunov method to improve damping of power swings by control of UPFC," *Proc. Inst. Elect. Eng., Gen., Transm. Distrib.*, vol. 151, pp. 252–260, Mar. 2004.
- [11] Z. Zhong, C. Xu, B. J. Billian, L. Zhang, S. J. Tsai, R. W. Conners, V. A. Centeno, A. G. Phadke, and Y. Liu, "Power system frequency monitoring network (FNET) implementation," *IEEE Trans. Power Syst.*, vol. 20, no. 4, pp. 1914–1921, Nov. 2005.
- [12] L. Dong, M. L. Crow, Z. Yang, and S. Atcitty, "A reconfigurable FACTS system for university laboratories," *IEEE Trans. Power Syst.*, vol. 19, no. 1, pp. 120–128, Feb. 2004.
- [13] P. Sauer and M. A. Pai, *Power System Dynamics and Stability*. Upper Saddle River, NJ: Prentice-Hall, 1998.
- [14] W.-H. Chen, D. J. Balance, and P. J. Gawthrop, "Optimal control of nonlinear systems: A predictive control approach," *Automatica*, vol. 39, pp. 633–641, 2003.
- [15] J. H. Chow, R. Galarza, P. Accari, and W. W. Price, "Inertial and slow coherency aggregation algorithms for power system dynamic model reduction," *IEEE*

Trans. Power Syst., vol. 10, no. 2, pp. 680–685, May 1995.

- [16] S. Geeves, “A modal-coherency technique for deriving dynamic equivalents,” IEEE Trans Power Syst., vol. 3, no. 1, pp. 44–51, Feb. 1998.
- [17] M. L. Ourari, L.-A. Dessaint, and V.-Q. Do, “Dynamic equivalent modeling of large power systems using structure preservation technique,” IEEE Trans. Power Syst., vol. 21, no. 3, pp. 1284–1295, Aug. 2006.
- [18] J. H. Chow, Ed., Time-Scale Modeling of Dynamic Networks With Applications to Power Systems. Berlin, Germany: Springer-Verlag, 1982.
- [19] G. Rogers, Power System Oscillations. Norwell, MA: Kluwer, 2000.
- [20] E. V. Larsen, J. J. Sanchez-Gasca, and J. H. Chow, “Concepts for design of FACTS controllers to damp power swings,” IEEE Trans. Power Syst., vol. 10, no. 2, pp. 948–956, May 1995.
- [21] P. Pourbeik and M. J. Gibbard, “Simultaneous coordination of power system stabilizers and FACTS device stabilizers in a multimachine power system for enhancing dynamic performance,” IEEE Trans. Power Syst., vol. 13, no. 2, pp. 473–479, May 1998.
- [22] N. Martins and L. T. G. Lima, “Determination of suitable locations for power system stabilizers and static VAR compensators for damping electromechanical oscillations in large scale power systems,” IEEE Trans. Power Syst., vol. 5, no. 4, pp. 1455–1469, Nov. 1990.
- [23] B. K. Kumar, S. Singh, and S. Srivastava, “Placement of FACTS controllers using modal controllability indices to damp out power system oscillations,” Proc. Inst. Eng. Technol., Gen., Transm., Distrib., vol. 1, no. 2, pp. 252–260, Mar. 2007.
- [24] C. Schauder and H. Mehta, “Vector analysis and control of advanced static VAR compensators,” Proc. Inst. Elect. Eng., C, vol. 140, no. 4, 1993.
- [25] M. Zarghami and M. L. Crow, “Discussion of effective control of interarea oscillations by UPFCs,” presented at the 39th North American Power Symp., Las Cruces, NM, Oct. 2007.



M Praveen Kumar received B.Tech Degree in Electrical & Electronics Engg. from JNT University, Hyderabad, India. Presently he is with Annamacharya Institute of Technology & Sciences, Rajampet, A.P,India, in Dept. of EEE and pursuing his M.Tech. His research interests includes power systems, FACTS,



P.B Chennaiah received B.Tech Degree in Electrical & Electronics Engg. from JNT University, Anantapur, India. M..Tech degree in electrical engineering from JNT University,Hyderabad. Presently he is with Annamacharya Institute of Technology & Sciences, Rajampet, A.P,India, in Dept. of EEE as an Associate professor. His research includes optimization techniques in power systems, FACTS,